UNIVERSITY OF CALIFORNIA, SAN DIEGO

Biochemical Properties of IKK and Bcl3

A Thesis submitted in partial satisfaction of the requirements for the degree Master of Science

in

Chemistry

by

Daniel Young Kim

Committee in charge:

Professor Gourisankar Ghosh, Chair
Professor Rommie Amaro
Professor Simpson Joseph

2016

This Thesis of Daniel Young Kim is approved, and it is acceptable in quality and form for publication on microfilm and electronically:

_____

_____

_____

Chair

University of California, San Diego

2016

DEDICATION

I dedicate this to my parents, who have offered unwavering support and encouragement throughout my education. I could not have done this without them.

TABLE OF CONTENTS

LIST OF FIGURES

PREFACE

This thesis is the final work of my Masters study at the University of California, San Diego. It serves as documentation of my research during the study, which has been made from October 2013 until March 2016. It presents the results of a study towards uncovering structural information of IKK complex.

ACKNOWLEDGEMENTS

I would like to give thanks to all the people who have helped me throughout my work. First, I would like to thank my mother and father for their love and unconditional support. Dr. Gourisankar Ghosh for providing me the opportunity to work on several amazing projects. Dr. Marie Mulero-Roig for her immense help and support and providing help whenever necessary. And finally, the rest of G.Ghosh lab members for all the aide they have provided.

ABSTRACT OF THE THESIS

Biochemical Properties of IKK and Bcl3

by

Daniel Young Kim

Masters of Science in Chemistry

University of California, San Diego, 2016

Professor Gourisankar Ghosh, Chair

Nuclear factor kappa B (NF-κB) plays a crucial role in the regulation of inflammation and immune response. NF-κB is composed to five family members, RelA, RelB, cRel, p52, and p50, which form combinatorial homo- and heterodimers. In resting cells, NF-κB dimers remain inactive and bound to an inhibitor of NF-κB (IκB) protein. IκB Kinase (IKK) phosphorylates IκB leading to its degradation and release of NF-κB into the nucleus. The function of the ternary IKK complex (IKK1, IKK2, NEMO) and the mechanism of NF-κB activation is not known. In an effort to understand the structure, the IKK complex has been expressed and isolated in insect, *E. coli*, and mammalian cells. However, full length wild type IKK proteins do not form a stable complex post-

overexpression and are difficult to purify. This suggests that aberrant post-translational modifications in the overexpression system might alter the stability of the native complex.

B-cell lymphoma 3-encoded protein (Bcl3) is an atypical IκB which binds to DNA:p52 and DNA:p50 binary complexes ultimately repressing or activating DNA transcription. The phosphorylation sites which affect DNA binding are not well known. The phosphorylation sites Ser33, Ser114, and Ser446 known to be crucial for DNA binding were analyzed through EMSA and wound healing assay. Results indicate that Ser114 is the critical residue in forming ternary complexes with DNA:p52 and DNA:p50 binary complexes. Our results elucidate the mechanism of how Bcl3 acts as a transcriptional regulator.

INTRODUCTION

NF-κB Family: In 1986, nuclear factor kappa B (NF-κB) was discovered by Sen and Baltimore as a DNA-binding transcription factor that recognizes the promoter for the gene responsible for encoding the immunoglobulin-kappa light chain in B cells. Whereas this early discovery found NF-κB as a constitutively expressed, active transcription factor in B cells, subsequent studies found it to be an inducible heterodimeric transcription factor in most cell types. NF-κB is a heterodimer composed of p50 kDa (p50) and 65 kDa (p65) polypeptides. Upon analysis of the cDNAs, p50 and p65 were found to be homologous at their N-terminal domain spanning roughly 300 residues. Both were found to be homologous to another transcription factor, cRel, discovered in 1982. The homologous N-terminal domain was named Rel Homology Domain (RHD). Two other family members, p52 and RelB, were subsequently discovered. These five proteins comprise the NF-κB family and can form transcriptionally active combinatorial homo- and heterodimers (Figure 1.1, Hayden et al., 2012).

During the cloning of the cDNAs encoding p50 and p52 polypeptides, it became clear that these polypeptides are generated from larger precursors, called p105 and p100, respectively. Functional and crystal structure analyses of NF-κB dimers have shown that the N-terminal RHD folds into two separate domains, RHD-N and RHD-C, which are connected by a flexible short peptide. RHD-N and the linker peptide are responsible for making DNA sequence specific contacts and RHD-C is responsible for subunit dimerization. The RHD-C also makes non-specific DNA contacts. P50 and p52 do not contain a transcriptional activation domain (TAD) and are unable to activate transcription as homodimers. The ability to initiate transcription is thus limited to the C-terminal TADs

of p65, c-Rel, and RelB. p50 and p52, however, can also positively regulate transcription without TADs through heterodimerization with NF-κB subunits containing TAD. All NF-κB factors contain a short basic peptide following its dimerization domain responsible for their nuclear localization. The basic peptide is referred to as the Nuclear Localization Signal (NLS) (Hayden et al., 2012).

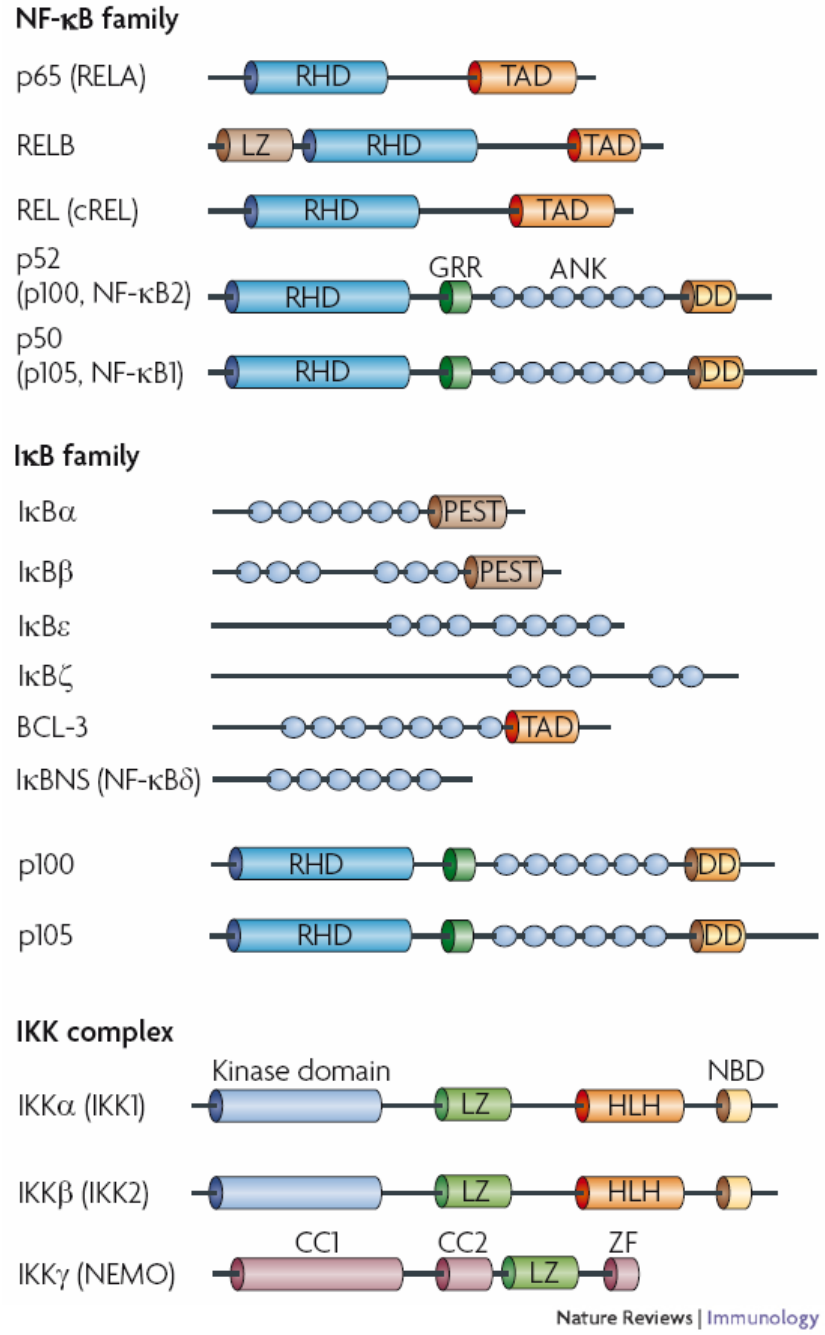

Figure 1.1: NF-κB Family Members, IκB Family Members, and IKK Complex (Ghosh and Hayden., 2008).

NF-κB Activation: In non B-cells, NF-κB is normally present in a latent (resting) state in the cytoplasm as an inhibited complex. An inhibitor of NF-κB (IκB) interacts stably with the NF-κB dimer blocking NF-κB's nuclear localization and DNA binding activity. Indeed, IκB directly contacts the NLS of NF-κB to sequester the complex within the cytoplasm. A large number of stimuli can activate NF-κB by inducing degradation of IκB. The key to this process is the activation of an IκB kinase (IKK). Active IKK phosphorylates IκB leading to its ubiquitination and degradation by the proteasome. NF-κB signaling pathways can be divided into two types: canonical and non-canonical pathways (Figure 1.2). The activation of both pathways share a common goal of activating the IKK and phosphorylation of IκB. Interestingly, induced NF-κB activates IκB among hundreds of other genes. Newly synthesized IκB can inactivate NF-κB by removing it from the DNA and exporting it to the cytoplasm. This negative feedback mechanism is critical to the hyperactivity of NF-κB (Hooper., 2006).

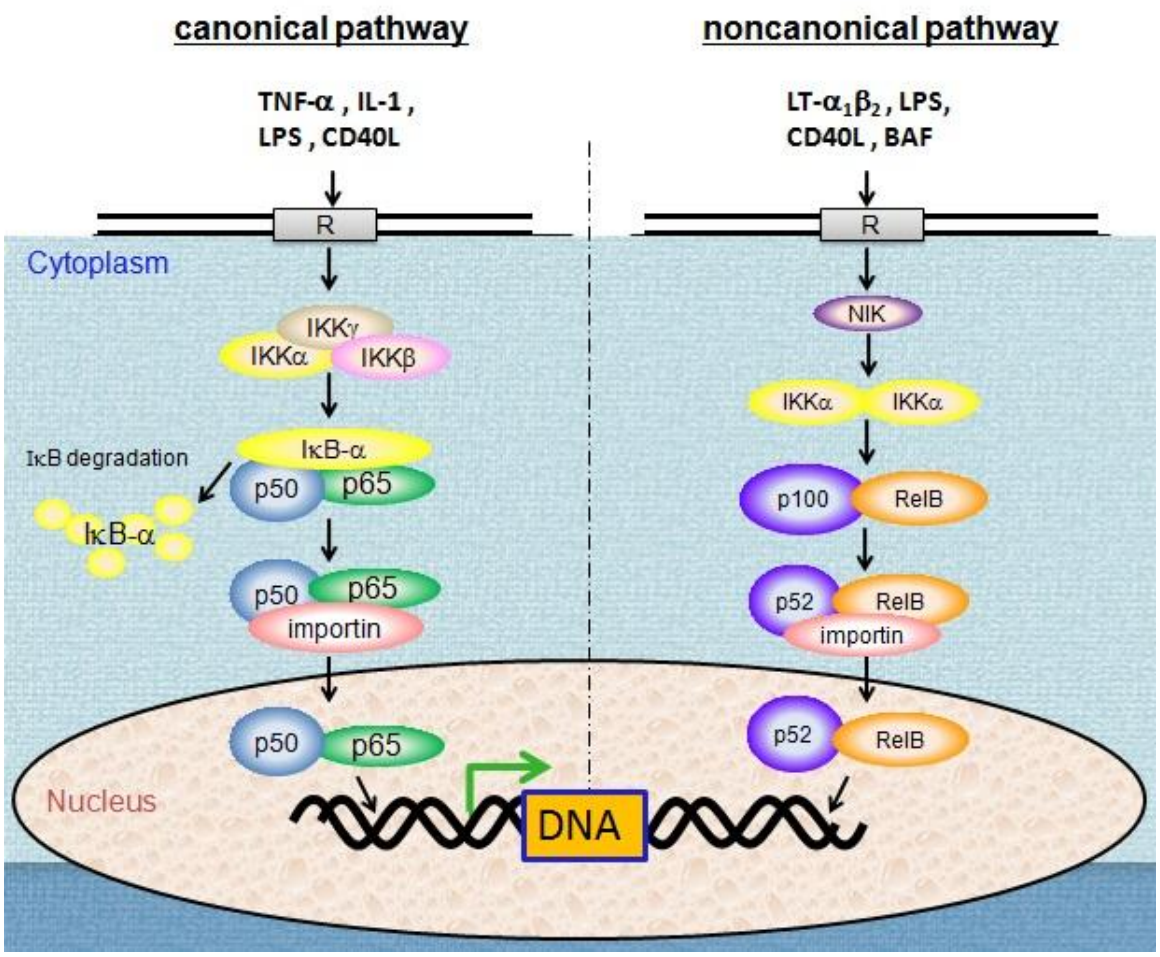

Figure 1.2: The canonical and noncanonical NF-κB activating pathways (Horie et al., 2012).

In the canonical pathway, the first step of signaling is the binding of a specific set of ligands to their cell surface receptors which leads to a cascade of reactions that finally act on IKK such that NF-κB dimers containing p65/RelA and cRel are activated. In the non-canonical pathway, a different set of stimuli is responsible for the activation IKK such that p52/RelB heterodimer is activated.

Genes & physiology: NF-κB activates or represses over five hundred genes ranging from cytokines, cell surface receptors, and transcription factors to anti-apoptotic and cell cycle (Hayden et al., 2012). NF-κB factors are therefore responsible for the regulation of diverse cell physiology. The most well studied of which is immune response and inflammation. Therefore, NF-κB's activity in immune cells is profound. NF-κB is also responsible for cell survival by inducing many anti-apoptotic factors. They are also critical for cell proliferation by activating many cell-cycle related genes (Hayden et al., 2012).

IκB Role: NF-κB remains inactive in the cell due to the suppression of its NLS by the binding of an IκB. There are three categories of IκB: prototypical inhibitors, precursor inhibitors, and atyptical inhibitors. The prototypical IκB consists of IκBα, IκBβ, and IκBε which bind to RelA (p65) and c-Rel dimers. The precursor IκB consists of p100 and p105. p100 inhibits all NF-κB members but prefers to bind to RelB. p105, on the other hand, inhibits all NF-κB family members except RelB. Finally, the atypical IκBs: Bcl3 and IκBζ, can form ternary complexes with p50 and p52 homodimers and regulate transcriptional activities on DNA (Hayden et al., 2012).

IκBα is the most extensively studied member of IκB. In the canonical pathway, IκBα binds to the p50/p65 NF-κB heterodimer to inhibit the complex. IκBα:p65:p50 complex is able to move between cytoplasm and nucleus by hiding the p65 derived NLS through IκBα's nuclear export signal. DNA binding is thus prevented until proteasomal degradation of IκBα which leads to the nuclear localization of NF-κB (Hayden et al., 2012).

Precursor inhibitor p105 is processed into releasing NF-κB family p50 from its N-terminus. The C-terminus contains ankyrin repeat domains which are normally responsible for cell differentiation and cell cycle control (Liou, H C et al., 1992). IκBα and IκBβ also have a homologous ankyrin repeat domain on the c-terminus. Unlike the prototypical inhibitors, p105 has been shown to prevent p50 homodimer from binding to a κB motif while minimally affecting the binding of p65.

Bcl3: B-cell Lymphoma 3-encoded protein (Bcl3) is an IκB which was discovered as a gene involved in chronic lymphocytic leukemia. Bcl3 is a member of the IκB family which forms stable complexes with NF-κB transcription factors. IκB proteins contain three structural regions: The central region contains six to seven ankyrin repeats that fold into the ankyrin repeat domain (ARD). The ARD provides the primary contact surface for NF-κB binding. Unlike classical IκB proteins (IκBα, -β and –ε) which prefer RelA or cRel containing NF-κB dimers for binding, Bcl3 shows preference towards NF-κB p50 or p52 homodimers. Besides the NLS, the N-terminus of Bcl3 is featureless. Serine and proline rich C-terminus is apparently flexible. Earlier reports revealed conflicting Bcl3 functions. Some reports showed that Bcl3 dissociates NF-κB p50 or p52 homodimer from bound DNA sequences, thereby functioning as a direct repressor of transcription (Franzoso et al., 1993; Franzoso et al., 1992; Wulczyn et al., 1992). Other reports demonstrated opposite function in that Bcl3 could associate with DNA-bound p50 or p52 homodimer forming transcriptional activation complex (Bours et al., 1993; Dechend et al., 1999; Fujita et al., 1993). We reported that Bcl3 functions both as co-activator and co-repressor of p52 dictated by DNA sequences of target genes. As few as

single base pair difference can determine if the p52: Bcl3 would act as an activator or repressor of transcription (Wang et al., 2012).

In cancer cells as well as transiently transfected cells, Bcl3 is present predominantly in the nucleus. This finding led to the mistaken assumption that Bcl3 is a nuclear protein. An NLS has been identified in its N-terminal region (Zhang et al., 1994). In many non-cancer cell types, such as erythroblasts, hepatocytes, and keratinocytes, Bcl3 primarily resides in the cytoplasm and requires activation prior to nuclear translocation (Brasier et al., 2001; Massoumi et al., 2006; Zhang et al., 1998). However, the signals that induce Bcl3 nuclear translocation are unknown.

Bcl3 was found to be extensively phosphorylated in different cell types (Bundy and McKeithan, 1997; Caamano et al., 1996; Nishikori et al., 2005; Viatour et al., 2004b). Earlier studies revealed that differential phosphorylation of Bcl3 was key to its distinct biochemical activities. Recombinant Bcl3 derived from bacteria and baculovirus with little or no phosphorylation had classical IκB-like activity that removed p50 and p52 homodimers from the DNA (Fujita et al., 1993). Later studies showed that Bcl3 expressed in mammalian cells formed ternary complexes with DNA:p50 or DNA:p52 binary complexes (Wang et al., 2012; Westerheide et al., 2001). Only two possible Bcl3 phosphorylation sites, Ser394 and Ser398, identified by consensus sequence-based prediction method were thought to be phosphorylated by GSK3β. These two sites are apparently required for Bcl3 degradation through the proteasomal pathway (Viatour et al., 2004a; Viatour et al., 2004b). However, there is no direct demonstration if these sites are indeed phosphorylated in the cell.

IKK Complex: It became clear that the IκB inhibitors undergo degradation in response to extracellular stimuli to release NF-κB. It was thought that a protein kinase must be activated in response to stimuli leading to phosphorylation-mediated degradation of IκB. Many of the serines, threonines and tyrosines could possibly undergo phosphorylation, but mutation of two N-terminal serines, Ser32 and 36, to alanines completely inhibited IκBα degradation and NF-κB activation. These findings led to the purification of an IκBα Ser32/36 specific kinase from TNFα activated HeLa cells. A kinase named IkappaB Kinase (IKK) was discovered that specifically phosphorylated IκBα Ser32 and 36 *in vitro*.

Further characterization of IKK revealed that IKK is not a single polypeptide protein but is composed of three subunits; two catalytic subunits, IKK1 and IKK2, and one adapter subunit, NEMO. Identification cDNA revealed that IKK1 and IKK2 possess similar primary structures with 50% sequence identity. Activation of the IKK complex was discovered to be the defining event in the regulation of NF-κB transcriptional activity.

IKK1 and 2 belong to the serine/theronine class of protein kinases, although mutation of serines 32 and 36 to threonines completely abolish NF-κB activation suggesting IKK is a serine-specific kinase. Gene knockout studies showed that IKK2 is specific to the canonical pathways and is activated by inducers such as TNFa, IL-1b and LPS. In addition to IκBα, activated IKK2 phosphorylates homologous serines located in the N-terminus of IκBβ and IκBε and two C-terminal serines in p105. The inducers of non-canonical pathway such as LTb, CD30 and BAFF activate IKK1. Once activated,

IKK1 phosphorylates the serines located in the C-terminal region of p100 leading to its processing into p52. These phosphorylations lead to their degradation and release of NF-κB.

NEMO is the non-catalytic subunit of the IKK complex required for the canonical NF-κB pathway activation. Barring a Zn-finger domain in the C-terminus, most of NEMO adopts coiled coil structure. The N-terminal part of the coiled coil forms a dimer and interacts with the C-terminal regions of IKK1 and IKK2 forming a parallel four helix bundle (Rushe et al., 2008).

The primary structure of IKK1 and IKK2 can be divided into four parts: from N- to C-termini these are a kinase domain (KD), a ubiquitin-like domain (UbL), long coiled coil helical domain and NEMO binding domain (NBD). Recent structures of IKK2 revealed that the helical domain forms a three helix bundle that holds the UBL and KD in the one end and self assemble (dimerize) on the other end. Since the native IKK contain all three subunits suggest that IKK1 and IKK2 forms a heterodimer suing their homologous dimerization domain.

In 1996, it was shown that NEMO was activated through a non-degradative Lysine-63 linked polyubuiquitination (Chen, Z). Lys63-linked polyubiquitin chains are formed by TRAF6, an E3 ligase, associating with a dimeric E2 complex. Ubiquitination of NEMO has been shown to be crucial to the activation of IKK. There are several different stimuli responsible for the Lys63-linked polyubiquitination. Later it became clear that Lys63-linked polyubiquitin chains are targeted by NEMO leading to its ubiquitination leading to the activation of IKK. Ubiquitinated NEMO recruits TAK1 which phosphorylates IKK2 on its activation loop serines, activating IKK2. Inhibitor IκB

is then phosphorylated and subsequently polyubiquitinated through Lysine 48-linked polyubiquitin chains and degraded by the 26S proteasome. Recent experiments have shown that in addition to Lys63-linked poly Ub chain, linear N- to – C linked Ub-chanin can also activate IKK2.

NEMO is frequently mutated in several human diseases. The gene sequence analysis identified several mutations mostly concentrated in the C-terminal in the leucine zipper (LZ) and Zn-finger domains. The LZ domain is the site of poly Ub chains. X-ray structures of Lys63 and linear di-Ub bound to the LZ domain explained how various pathogenic mutations might be able to block Ub chain binding. It is unclear how ubiquitination of NEMO allows intramolecular interactions between the Ub chain and LZ domain. It is also not known how this binding event induces IKK2 activation. The focus of this study is to explore the molecular determinants of IKK2 activation by NEMO in context of the IKK holocomplex.

MATERIALS AND METHODS

Insect Cell Protocols

SF9 Viral Stock Construction and Transfection: The desired sequences were cloned into pFastBac Expression Vector and transformed into DH10alpha *E. coli* and sequenced. The clones were then transformed into DHA10Bac *E. coli* into plates containing kanamycin, gentamicin, tetracyclin, Bluo-gal, and IPTG and screened using blue-white colony after 48 hours incubation. The white colonies were then plated onto a fresh agar plate containing kanamycin, gentamicin, tetracyclin, Bluo-gal, and IPTG to confirm phenotype. The plasmid bacmid DNA was isolated and checked through PCR and sequencing.

The P1 viral stock was created by infecting SF9 cells at 0.8 million cells/mL on a 6-well plate with Cellfectin, unsupplemented SF-900 media, and dilute baculovirus DNA following the Bac-to-Bac Thermofisher protocol . The supernatant was collected 72 hours post-transfection. A P2 viral stock was created by amplifying the viral stock through another infection of SF9 cells at 0.5 million cells/mL in 10 cm plates and collecting the supernatant after 72 hours. From this stock the transfection was optimized through several dilutions and analyzing with Western Blots. The best expression ratio was chosen for larger scale expression and transfected in suspension.

SF9 Cell Lysis: SF9 cells were collected and spun down at 5000 rpm for 10 min at 4°C. The supernatant was aspirated and the pellet was resuspended in lysis buffer (10 mM Hepes pH 8.0, 250 mM NaCl, 1 mM EDTA, 0.5% NP-40, 0.2% Tween, 1 mM DTT,

1MM PMSF). After 5 minutes on ice, the lysis mixture was spun at 13,000 rpm for 10 min at 4C and the supernatant cell lysis was kept for further purification.

TEV treatment: TEV-protease was added 1:100 w/w to protein and digested overnight at 4 C. 0.5 mM ATP was added to solubilize mixture next day at 30C for 1.5 hours.

E. coli Protocols

Miniprep Protocol for Plasmid DNA purification from Bacteria: 2 mL of bacterial culture was grown overnight in an eppie tube from a single colony. Cells were pelleted at 6000 rpm for 30 sec. LB media was aspirated and 300 μL of Solution 1 was added and mixed by test tube rack grating. (Make sure cells are well homogenized) Added 300 μL Solution 2 and slowly inverted tube 10 times. Keep at room temperature between 4-5 minutes but no longer. Added 300 μL Solution 3 to neutralize the lysis and kept on ice between 9-10 minutes. Pelleted at max speed for 10 min and transferred supernatant. Added 800 μL isopropanol and inverted tube 10 times and kept at room temperature for 15 minutes. Pelleted DNA at max speed for 10 min and removed supernatant. Added 500 μL cold 70% ethanol and vortexed for 10 seconds. Spun max speed and removed supernatant. Spun again and removed remaining supernatant with a p10 pipet. Let tubes try on bench for 10 min. Resuspend DNA in 50 μL MilliQ H2O or TE.

Solution 1: Stored at 4C with fresh RNAse added each time. (50 mM Glucose, 25 mM Tris-Hcl pH 8.0, 10 mM EDTA pH 8.0)

Solution 2: Made fresh each time. (0.2 N NaOH, 1% SDS)

Solution 3: Stored at 4C (3 M Potassium Acetate, 2 M Acetic Acid)

Heat Shock Transformation: Thawed competent cell tubes on ice. Added 100 ng – 1 ug DNA (volume no larger than 1/5 of cell volume) and kept on ice 20 min. Heat shocked the cells in a 42C water bath for 45 sec and kept on ice for 5 min. Added 800 μL LB media to each tube and incubated at 37C for 1 hour.

Protein Expression: Cloned target DNA sequence into desired vector. Transformed vector into BL21 or BL21-Rosetta competent cells and plated onto agar plate with appropriate antibiotics + 0.37 mg/mL chloramphenicol. Left plate at 37C overnight. Picked single colonies the next day and inoculated into 5-20 mL of LB at 37C. Once the OD was in a visible log phase transferred to a larger media container (1 L or 2 L) and grew until 0.3 OD depending on protein. Added 0.1-0.4 mM IPTG to log phase cells and incubate at room temperature overnight. Spun cells at 3000 rpm for 30 min to collect cell pellet.

General Purification Protocols

Nickel Purification: Cell lysis was loaded onto a gravity flow Nickel column and washed with cell lysis buffer + 10 mM Imidazole for 10 column volumes or until the

Bradford reading was at 0.01 mg/mL or lower. Then the protein was eluted with lysis buffer + 500 mM Imidazole in 1 mL fractions or through batch elution.

Gel Filtration: Protein which has been through at least first step purification was loaded onto either a SD200 or Superose6 column connected to an FPLC and run using 20 mM Tris pH 8.0 or (Hepes pH 8.0), 50 mM NaCl, and 1 mM DTT. Fractions were collected based on chromatograph peaks.

Gravity Q-S Purification: Cell lysis in lysis buffer (20 mM Tris pH 8.0, 50 mM NaCl, 1 mM DTT) was loaded onto an S column which led to a Q column. The Q column was detached from the setup and was washed with lysis buffer until protein concentration from Bradford reading was at 0.01 mg/mL or lower. A gradient elution mixer in 20-30 fractions from 50 mM NaCl to 1 M NaCl.

Hi-trap Q Purification: Protein in lysis buffer (20 mM Tris pH 8.0, 50 mM NaCl, 1 mM DTT) was loaded onto column using a peristaltic pump. The column was washed with lysis buffer until Bradford reading was at 0.01 mg/mL. The column was attached to an FPLC and eluted into 20 column volumes. The peaks were collected and analyzed.

Mono Q Purification: Protein in lysis buffer (20 mM Tris pH 8.0, 50 mM NaCl, 1 mM DTT) was loaded onto column through an FPLC. The column was washed with lysis buffer for 10 column volumes and eluted into 20 column volumes. The peaks were collected and analyzed.

FLAG purification: Cell lysis was batch bound in FLAG resin overnight rotating at 4C. The resin was spun down at 1,000G for 5 min. The protein-bound resin was washed until the supernatant had a Bradford reading lower than 0.01 mg/mL. The resin was incubated in 3X FLAG peptide for 2 hours for elution. Two elution fractions were collected.

Mammalian Cell Protocols

Maintaining HEK 293T Cell Cultures: HEK 293T cell culture was grown in DMEM supplemented with 5% FBS and Penicillin, Streptomycin, and Glutamine. The cell lines were split to 10% confluency and split at 95% confluency onto treated plates.

Transfecting 293T Cell Cultures: HEK 293T cells were split to 30% confluency on plates. The cells (10 ug for 10 cm plates) were transfected using PEI and DNA cloned into pBABE expression vector the next day at 60% confluency. The cells were collected after 72 hours and lysed on ice for 10 min with RIPA Cell Lysis Buffer (20 mM Tris pH 8.0, 200 mM NaCl, 1% Triton-X100, 2 mM DTT, 5 mM 4-nitrophenyl phosphate di(Tris) Salt, 2 mM Na3VO4) with 1 mM PMSF and protease inhibitor cocktail added freshly.

Protocols for Electrophoretic Mobility Shift Assay

EMSA Probe Labeling: Mixed 4 pmol top stranded DNA, 10x PNK buffer, T4-PNK, and water to 19 μL and centrifuged to bottom of eppie tube. Added 1 μL 32-gamma-ATP and incubated at 37C for 2 hours. Added 30 μL H2O to make a total of 50

μL. Prepped a MicroSpin G-25 column by resuspending resin by tapping the tube. Loosened the cap ¼ of a turn and snapped off bottom closure. Placed column in a eppie tube for support and spun the column 1 min at 735xg. Placed column in fresh 1.5 mL eppie tube and slowly applied sample to center of the angled surface of the compacted resin bed without disturbing resin. Spun column for 2 min at 735xg and discarded column. Added 1 μL 5M NaCl, 5 μL bottom stranded DNA from 1 pmol/μL stock. Placed on 95C heating block for 5 min. Placed on 37C heating block for 15 min. Added 100 μL H2O and pipetted up and down to mix. Stored at -20C.

EMSA Native Gel: Made a 5% Acrylamide, 5% Glycerol, 1x TGE (24.8 mM Tris Base, 190 mM Glycine, 1 mM EDTA) gel in a volume of 40 mL. Add 400 μL of fresh 10% APS and 20 μL TEMED to polymerize. Pre-ran the gel to make native at 200 V for 1 hour using 1x TGE buffer.

EMSA Binding Reaching and Running Gel: Counted hot probe and made sure count is 10,000 CPM. Mixed hot probe, protein/nuclear extract, 2x Binding Buffer, and Dilution buffer to a total of 6 μL 30 min before loading the gel. Loaded the gel with one lane of just hot probe and 10x DNA dye to prevent probe from running off the gel. Ran gel at 200V until DNA dye band was 1 inch above the bottom of gel or for 1 hour. Dried the gel and exposed the gel to a phosphoiimager overnight.

2x Binding Buffer: Keep at -20C (10 mM Tris-HCl pH 7.5, 50 mM NaCl, 10% Glycerol, 1% NP-40, 1 mM EDTA, 0.1 mg/mL PolydIdC)

Dilution Buffer: Keep at 4C and add 1 mM fresh DTT each time (10% Glycerol, 0.2 mg/mL BSA, 20 mM Tris pH 7.5, 50 mM NaCl)

Wound Healing/Scratch Assay: Cells were split to 80% confluency on an untreated 24-well plate and grown to 100% confluency overnight. Then the plates were scratched with a p1000 tip down the center. Images were taken at 0, 24, and 48 hours at 10x magnification.

IKK RESULTS

Expression of IKK1 and IKK2 fusion proteins in SF9 cells: The IKK complex has been known to exist as a ternary complex *in vivo* (Zandi et al., 1997). However, the stoichiometric ratio of the subunits within the complex and the functional consequences of heterodimerization are not yet known. The x-ray crystal structure of the IKK2 homodimer has been previously characterized by Liu et al., 2013 and Xu et al., 2011, while three dimensional structures of the IKK1 subunit have been solved in our lab using both cryo-electron microscopy (cryo-EM) and X-ray crystallography (Polley at al. 2016, under review). A major challenge in investigating heterodimerization is that the complex has been difficult to crystallize. Furthermore, the strength of dimerization between IKK1 and IKK2 is unknown.

To ensure IKK1 and IKK2 dimerization, the dimerization domains of NF-κB p50 and p65 proteins, which are known to interact very tightly, were fused to IKK1 and IKK2, respectively, on the C-terminal domain which harbors a TEV cut site. Three glycine residues were added in between IKK1/2 and p50/p65 in order to allow some flexibility for the dimerization (Figure 2.1).

Figure 2.3 shows P2 viral expression of these hybrid proteins transfected in SF9 insect cells. Clone #3 of IKK1/p50 and Clone #1 of IKK2/p65 were chosen for further larger scale protein expression and purification with Nickel and gel filtration (Figure 2.3

and 2.4). However, the yield was too low (200 μg from 1L SF9 culture).

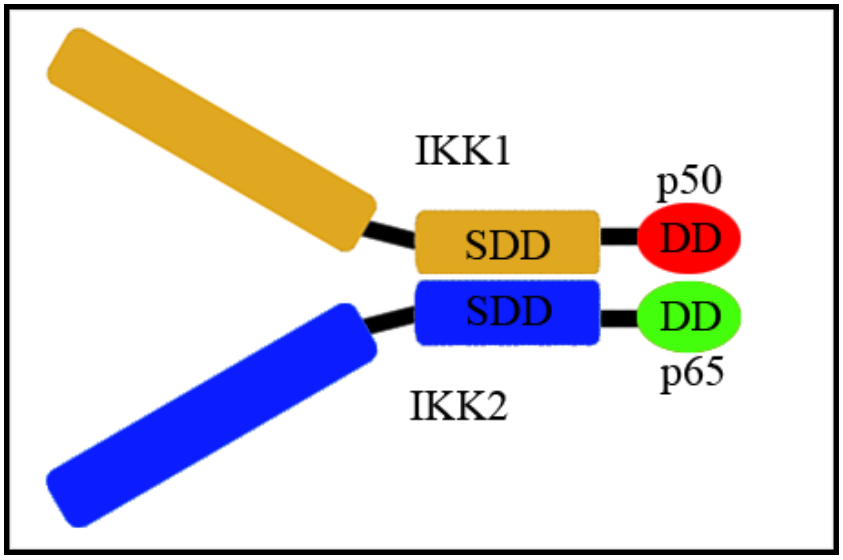

Figure 2.1: IKK1/p50 and IKK2/p65 fusion construct cartoon. The proteins are linked with three glycine residues.

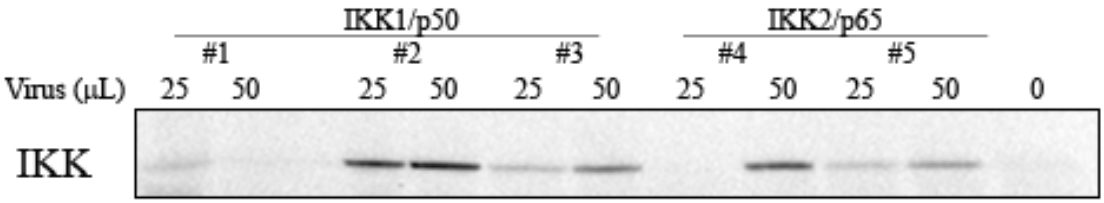

Figure 2.2: Verification of IKK1-p50 and IKK2-p65 fusion protein in bacculovirus P2 viral transfection optimization.

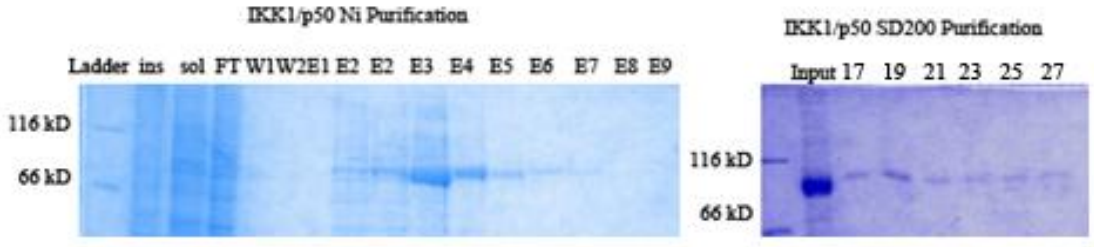

Figure 2.3: One liter of IKK1/p50 fusion protein Nickel purification followed by gel filtration.

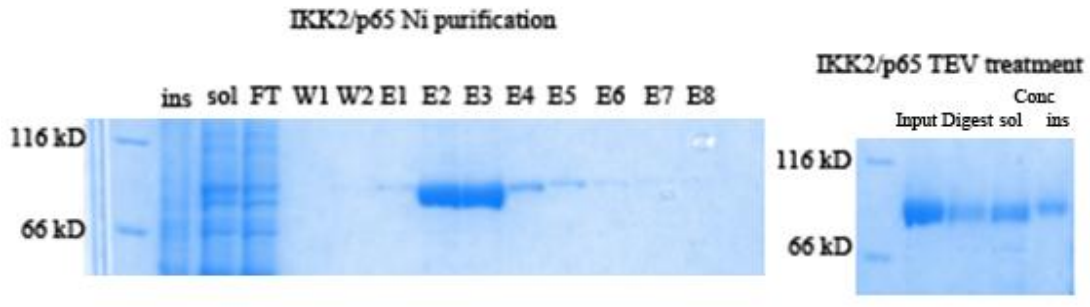

Figure 2.4: One liter of IKK2/p65 fusion protein Nickel purification followed by TEV treatment.

IKK2 FL WT and NEMO in SF9 cells: In efforts to characterize full length wild type IKK2 structure, the protein was cloned with a histidine tag , expressed in SF9 insect cells, and purified with Nickel-NTA affinity chromatography, followed by Superdex200 gel filtration (Figure 2.5 and 2.6). IKK2 peak fractions were concentrated and combined with NEMO and run through Superose6 gel filtration (Figure 2.7). The results indicated that the complex could be formed and was stable through gel filtration. Once again, the issue was that the yield was too low (undetectable through Bradford assay post-complex formation) through the SF9 insect cell expression system.

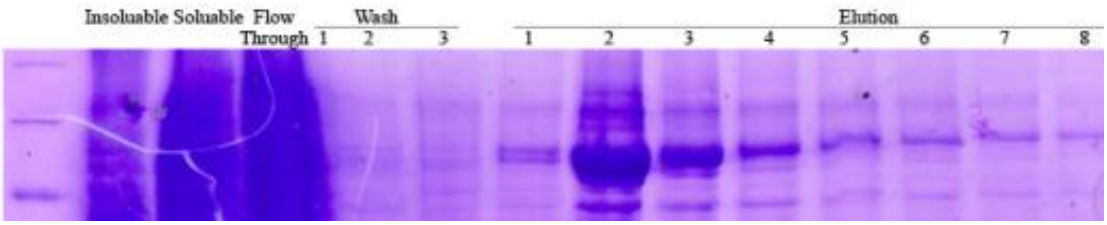

Figure 2.5: IKK2 full length wild type Nickel purification. Fraction 2-4 were collected for gel filtration.

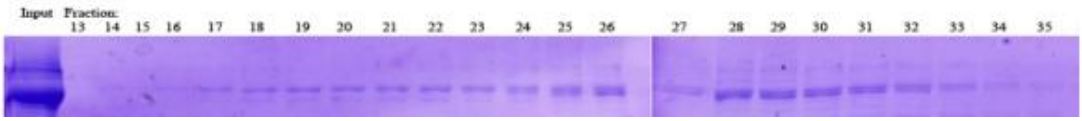

Figure 2.6: IKK2 FL WT SD200 gel filtration. Fractions 17-19 and 27-29 were collected and concentrated.

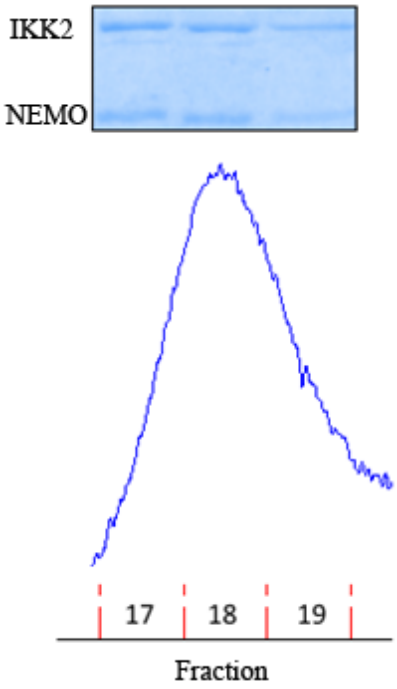

Figure 2.7: IKK2 FL WT was mixed with NEMO and run through Superose6 gel filtration. Both IKK2 and NEMO bands were found at a peak found between fractions 17-19.

IKK expression in *E. coli*: Next, the IKK2:NEMO complex was expressed in *E. coli* Rosetta cells (Figure 2.8). Though the protein yield was great in the cell lysis, most of the protein was found in the insoluble pellet after centrifugation (Figure 2.8). In order

to solubilize the protein, a refolding technique using 7M urea and rapid dilution was utilized. The protein did not did not refold after urea treatment (Figure 2.9). In addition, di-ubiquitin was added to stabilize the complex but no phosphorylation of IKK occurred (Figure 2.10). Several *E. coli* chaperone proteins (pKJE8, pGRO7, pKJE7, pTF2, pTF16) were used to aid in protein folding, but the protein remained mostly insoluble. The purified protein showed very little activity in comparison to its counterpart expressed in SF9 cells (Figure 2.11)

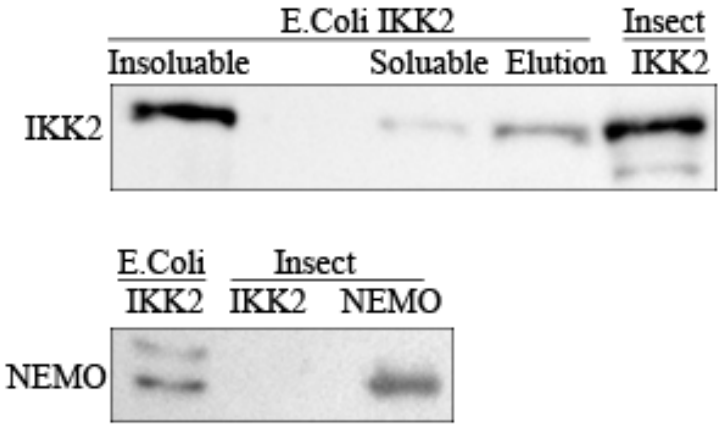

Figure 2.8: Testing expression of IKK2 and NEMO in *E. coli*.

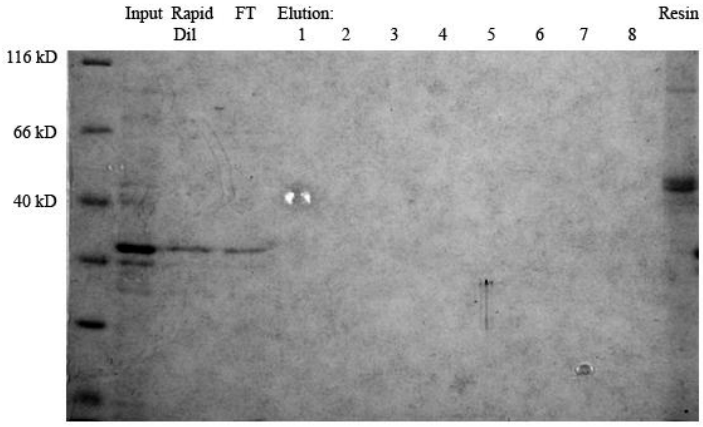

Figure 2.9: Refolding of IKK2 and NEMO complex in urea.

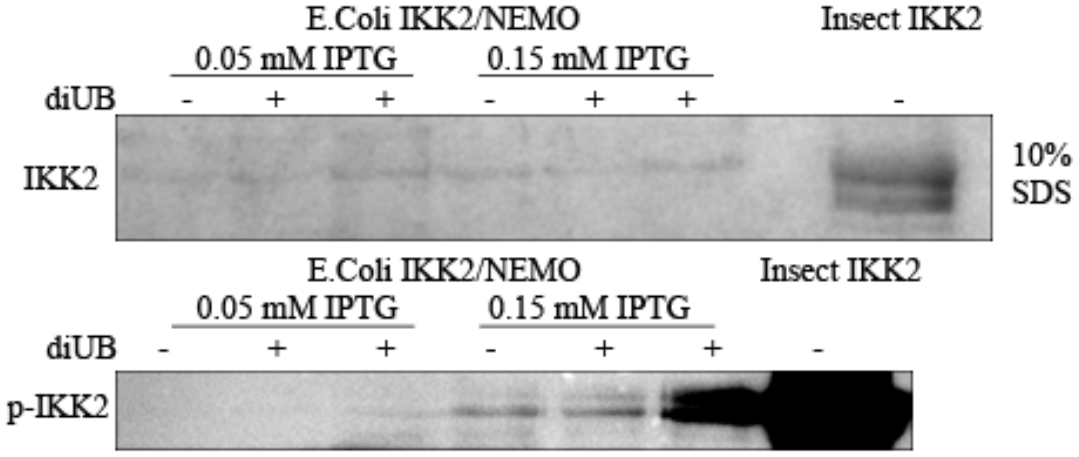

Figure 2.10: Addition of 1:1 w/w di-ubiquitin to *E. coli* coexpressed IKK2/NEMO to test if di-Ub NEMO can phosphorylate IKK2. Phospho-IKK2 antibody was used to check activity. Insect IKK2 used as control.

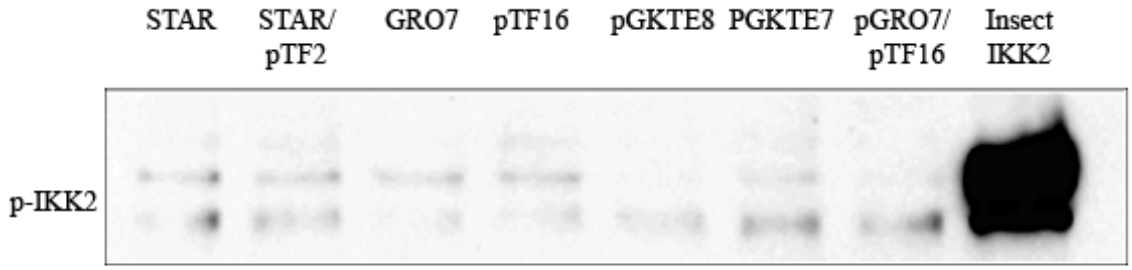

Figure 2.11: Testing the phosphorylation of *E. coli* derived IKK2 with the aid of chaperone proteins.

IKK expression in HEK 293T: The goal of characterizing IKK1 and IKK2 dimerization as well as IKK2 and NEMO complex was to obtain a model for the IKK holocomplex structure. In order to do so, we expressed full length IKK1, His-tagged IKK2, and FLAG tagged-NEMO in HEK 293T mammalian cells. Ebola viral protein

VP35 has been shown to induce high levels of recombinant proteins through transfected HEK-2 293T cells by Gantke et al., 2013. VP35 plasmid was added to the DNA transfection procedure. The full length complex was expressed and a subsequent FLAG immunoprecipitation (IP) showed enrichment of the whole complex (Figure 2.12). In order to further stabilize the complex, TNF-alpha (5 ng/mL) was added 1 hour post-lysis. The resulting FLAG IP followed by Nickel-NTA affinity purification revealed a IKK1, IKK2, and NEMO ternary complex (Figure 2.13), yet the total yield was very low (25 μg from fifty 10cm plates) with much of the protein lost in each purification step. FLAG purified IKK complex was loaded on Super6 gel filtration and resulted in an elution with several peaks corresponding to IKK1, IKK2, and NEMO (Figure 2.14). The ternary complex was then purified using High-trap Q and showed several peaks once again indicating that the complex was not stable and actually falling apart. One hypothesis is that overexpressing the IKK complex *in vivo* may cause the complex to become unstable and break apart.

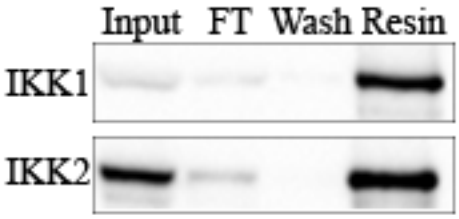

Figure 2.12: FLAG immunoprecipitation to investigate the formation of the IKK holocomplex..

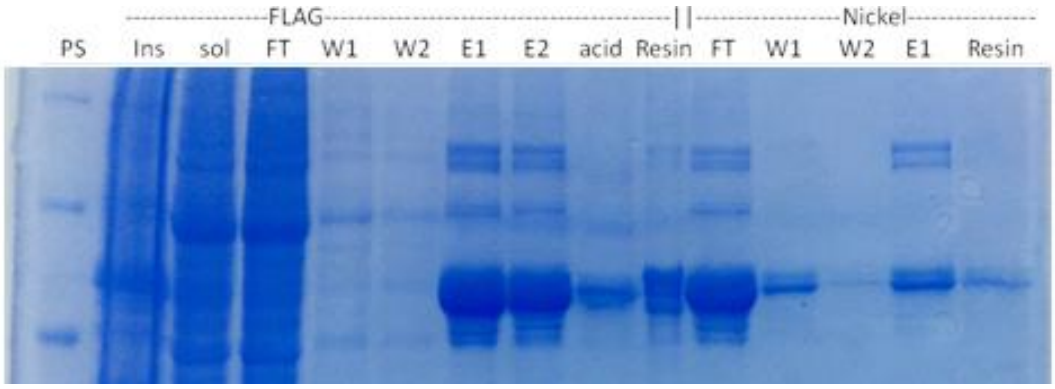

Figure 2.13: Large scale HEK293 IKK complex expression followed by FLAG and Nickel-NTA affinity purification.

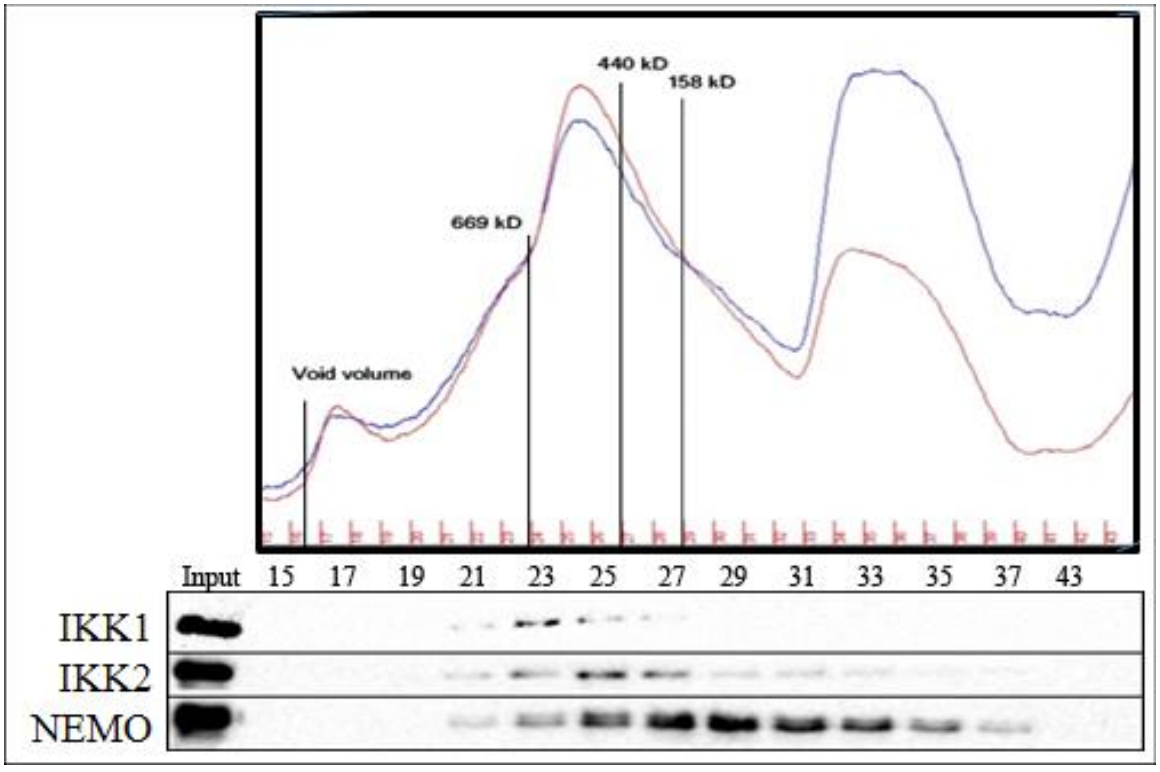

Figure 2.14: Superose6 gel filtration FLAG purified IKK complex and corresponding western.

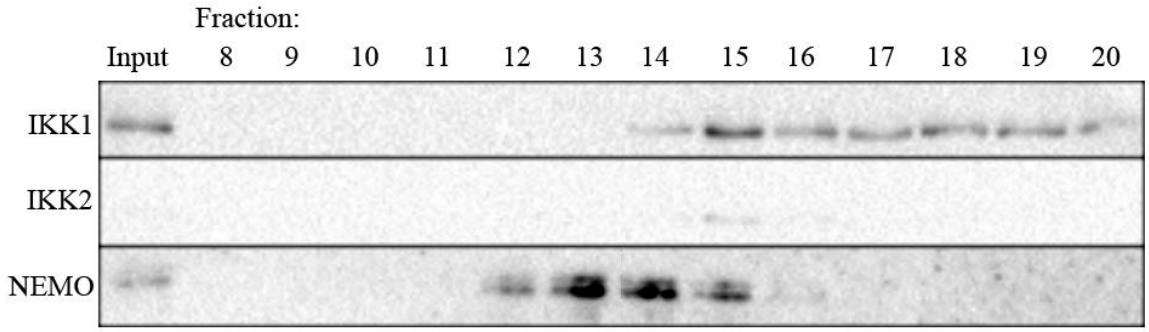

Figure 2:15: Western blot of High-trap Q purified IKK complex.

Bcl3 RESULTS

Bcl3 EMSA: We have shown that *E. coli* Expressed Bcl3 acts as an inhibitor of the p52:DNA complex. That is, the p52:Bcl3 complex cannot bind DNA. The research goals of the Ghosh laboratory is to identify the site(s) of Bcl3 phosphorylation required to convert Bcl3 into a transcription factor. In our laboratory, Dr. Vivien Wang showed that there are at least 15 sites in Bcl3 are phosphorylated in 293T cells. She further showed that phosphorylation of Serine 33 of Bcl3 is critical for its nuclear localization and phosphorylation of Serine 446 is critical for transcriptional activity of Bcl3. However, conversion of Ser33 and Ser446 into phospho-mimetic version glutamic acid was not sufficient to associate with the p52:DNA binary complex. Systematic changes of several other sites did not improve the transcriptional activity of the mutants as evaluated by luciferase assay with the exception of Ser114. I made glutamic acid mutation at position 114 in the context of Glu33 and Glu446. The Bcl3EEE triple mutant was expressed in *E. coli* and tested for ternary complex formation with the p52:DNA and p50:DNA complexes by EMSA. Figure 3.1 shows that both p52 and p50 DNA binding activity is disrupted by addition of wild type (unmodified) Bcl3. In contrast, the S33/114/446E makes a clear ternary complex with p52 and DNA. The EEE triple mutant also forms a ternary complex with p50 and DNA. I further tested if Bcl3 and p52 (or p50) are present in the ternary complex by antibody supershift. As shown in figure 31. Both Bcl3 and p52 (and p50) shift the complex ternary complex conforming the integrity of the complex. I conclude that phosphorylation at all three sites are important for the complex formation with p50 (and p52) with DNA. Interestingly, the ternary complex with p50 and DNA

does not appear to be as stable as that with p52 and DNA. This suggests that additional phosphorylation might be required for the full strength binding.

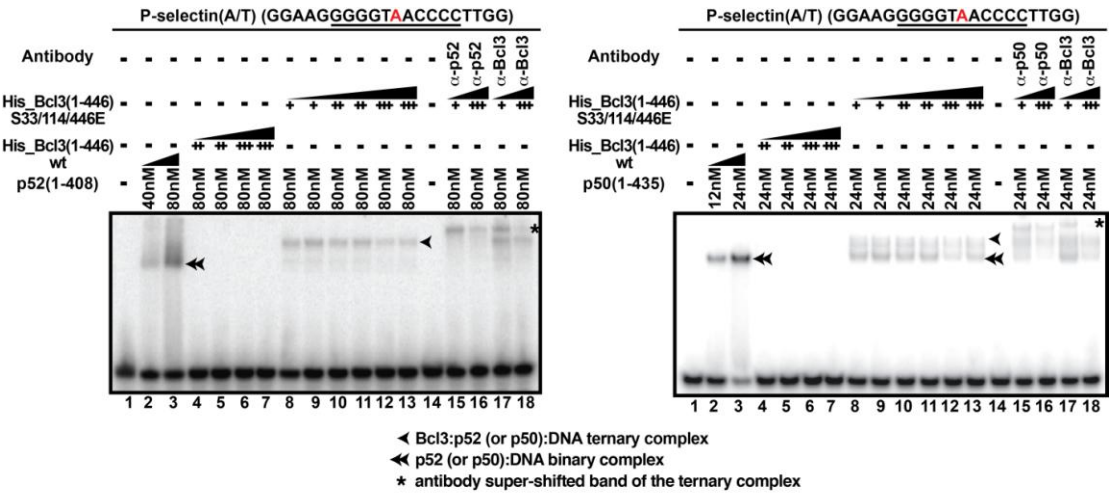

Figure 3.1: Bcl3 WT and S33/114/446E mutant EMSA with p50 and p65.

Bcl3 Scratch Assay (Cell migration): We wanted to test the role of phosphorylation *in vivo* activity of Bcl3. To test this we created alanine mutations at positions 114 and 446. We kept phospho-mimetic mutation at position 33 since nuclear localization is essential to carry out transcriptional function. The mutant E33/A114/A446 (Bcl3 EAA) was introduced in a Bcl3 knock down U2OS cells. In addition to the EAA triple mutant, we also introduced the E33/A446 double mutant and E33/E446 double mutants into the Blc3 KD U2OS cells. As control wt U2OS, (Bcl3 KD) U2OS, (Bcl3KD w/vector U2OS cells were used. The wound healing assay (scratch assay) involves creating a wound in a cell monolayer and capturing images over a time period to quantify migration rate of the cells. Cells expressing S33/114E mutant migrate much faster than wild type U2OS cells. Cells expressing the S33E/S114/446E triple mutant do not seem to

show much migration even after two days. But Bcl3 KD and KD with vector did not recover even after two days of scratch. The EA double mutant showed an intermediate defect. These results suggest that defect in transcription activity of Bcl3 result in defective cell migration.

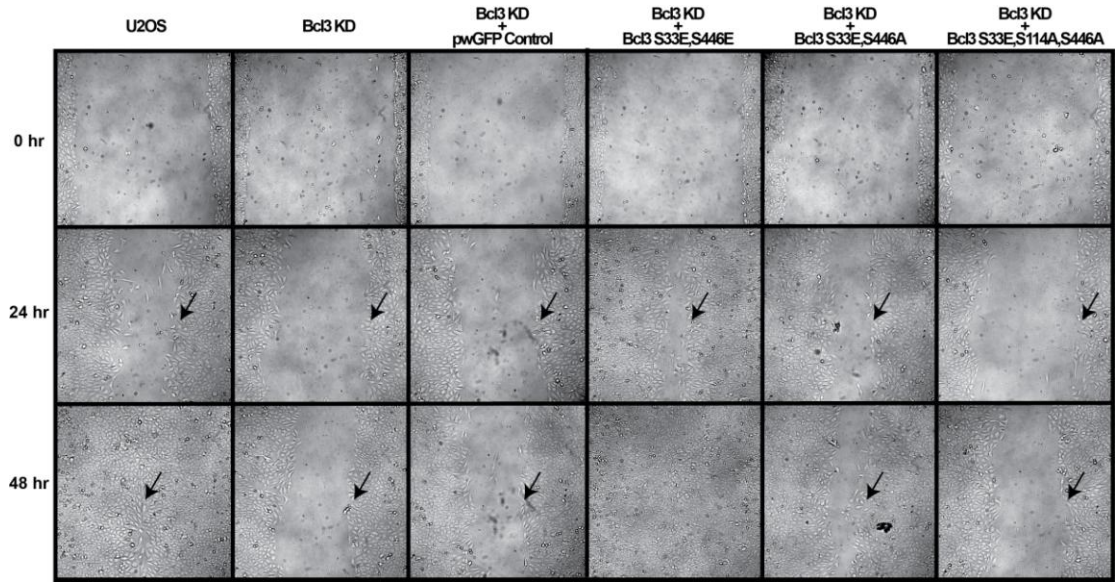

Figure 3.2: Wound healing assay of U2OS, Bcl3-KD, Bcl3-KD empty vector, EE mutant, EA mutant, and EAA mutant.

REFERENCES

Bours, V. "The Oncoprotein Bcl-3 Directly Transactivates through κB Motifs via Association with DNA-binding P50B Homodimers." Cell 72.5 (1993): 729-39. Print.

Brasier, A. R. "NF-kappa B-inducible BCL-3 Expression Is an Autoregulatory Loop Controlling Nuclear P50/NF-kappa B1 Residence." Journal of Biological Chemistry 276.34 (2001): 32080-2093. Print.

Bundy, D. L., and T. W. Mckeithan. "Diverse Effects of BCL3 Phosphorylation on Its Modulation of NF- B P52 Homodimer Binding to DNA." Journal of Biological Chemistry 272.52 (1997): 33132-3139. Print.

Chen, Zhijian J., Lana Parent, and Tom Maniatis. "Site-Specific Phosphorylation of IκBα by a Novel Ubiquitination-Dependent Protein Kinase Activity." Cell 84.6 (1996): 853-62. Web.

Dechend, Ralf, Fuminori Hirano, Kerstin Lehmann, Vigo Heissmeyer, Stephane Ansieau, F. Gregory Wulczyn, Claus Scheidereit, and Achim Leutz. "The Bcl-3 Oncoprotein Acts as a Bridging Factor between NF-κB/Rel and Nuclear Co-regulators." Oncogene 18.22 (1999): 3316-323. Print.

Hayden, M. S., and S. Ghosh. "NF- B, the First Quarter-century: Remarkable Progress and Outstanding Questions." Genes & Development 26.3 (2012): 203-34. Web.

Hooper, Claudie. "Overview of NF-kB Signaling." Overview of NF-kB Signaling. Abcam, n.d. Web. 09 Mar. 2006.

Franzoso, G., Bours, V., Azarenko, V., Park, S., Tomita-Yamaguchi, M., Kanno, T., … Siebenlist, U. (1993). The oncoprotein Bcl-3 can facilitate NF-kappa B-mediated transactivation by removing inhibiting p50 homodimers from select kappa B sites. The EMBO Journal, 12(10), 3893–3901.

Fujita, T., G. P. Nolan, H. C. Liou, M. L. Scott, and D. Baltimore. "The Candidate Proto-oncogene Bcl-3 Encodes a Transcriptional Coactivator That Activates through NF-kappa B P50 Homodimers." Genes & Development 7.7b (1993): 1354-363. Print.

Gantke, Thorsten, Sabrina Boussouf, Julia Janzen, Nicholas A. Morrice, Steven Howell, Elke Mühlberger, and Steven C. Ley. "Ebola Virus VP35 Induces High-level Production of Recombinant TPL-2–ABIN-2–NF-κB1 P105 Complex in Co-transfected HEK-293 Cells." Biochem. J. Biochemical Journal 452.2 (2013): 359-65. Print.

Ghosh, Sankar, and Matthew S. Hayden. "New Regulators of NF-κB in Inflammation." Nat Rev Immunol Nature Reviews Immunology 8.11 (2008): 837-48. Print.

Horie, Kana. "Inhibition of Canonical NF-kappaB and Suppression of Inflammation and Cancer Growth by Designed Inhibitor DHMEQ."Eoncosurg (2012): n. pag. Web. 15 Mar. 2016.

Liou HC, Nolan GP, Ghosh S, Fujita T, Baltimore D. The NF-kappa B p50 precursor, p105, contains an internal I kappa B-like inhibitor that preferentially inhibits p50. The EMBO Journal. 1992;11(8):3003-3009.

Massoumi, Ramin, Katarzyna Chmielarska, Katharina Hennecke, Alexander Pfeifer, and Reinhard Fässler. "Cyld Inhibits Tumor Cell Proliferation by Blocking Bcl-3-Dependent NF-κB Signaling." Cell 125.4 (2006): 665-77. Print.

Nishikori, Momoko, Hitoshi Ohno, Hironori Haga, and Takashi Uchiyama. "Stimulation of CD30 in Anaplastic Large Cell Lymphoma Leads to Production of Nuclear Factor-kappaB P52, Which Is Associated with Hyperphosphorylated Bcl-3." Cancer Science 96.8 (2005): 487-97. Print.

Rushe, Mia, Laura Silvian, Sarah Bixler, Ling Ling Chen, Anne Cheung, Scott Bowes, Hernan Cuervo, Steven Berkowitz, Timothy Zheng, Kevin Guckian, Maria Pellegrini, and Alexey Lugovskoy. "Structure of a NEMO/IKK-Associating Domain Reveals Architecture of the Interaction Site." Structure 16.5 (2008): 798-808. Print.

Viatour, Patrick, Marie-Paule Merville, Vincent Bours, and Alain Chariot. "Protein Phosphorylation as a Key Mechanism for the Regulation of BCL-3 Activity." Cell Cycle 3.12 (2004): 1498-501. Print.

Viatour, Patrick, Emmanuel Dejardin, Michael Warnier, Florence Lair, Estefania Claudio, Fabrice Bureau, Jean-Christophe Marine, Marie-Paule Merville, Ulrich Maurer, Douglas Green, Jacques Piette, Ulrich Siebenlist, Vincent Bours, and Alain Chariot. "GSK3-Mediated BCL-3 Phosphorylation Modulates Its Degradation and Its Oncogenicity."Molecular Cell 16.1 (2004): 35-45. Print.

Wang, Vivien Ya-Fan, Wendy Huang, Masataka Asagiri, Nathanael Spann, Alexander Hoffmann, Christopher Glass, and Gourisankar Ghosh. "The Transcriptional Specificity of NF-κB Dimers Is Coded within the κB DNA Response Elements." Cell Reports 2.4 (2012): 824-39. Print.

Westerheide, S. D., M. W. Mayo, V. Anest, J. L. Hanson, and A. S. Baldwin. "The Putative Oncoprotein Bcl-3 Induces Cyclin D1 To Stimulate G1 Transition." Molecular and Cellular Biology 21.24 (2001): 8428-436. Print.

Wulczyn, F. Gregory, Michael Naumann, and Claus Scheidereit. "Candidate Proto-oncogene Bcl-3 Encodes a Subunit-specific Inhibitor of Transcription Factor NF-κB." Nature 358.6387 (1992): 597-99. Print.

Zandi, Ebrahim, David M. Rothwarf, Mireille Delhase, Makio Hayakawa, and Michael Karin. "The IκB Kinase Complex (IKK) Contains Two Kinase Subunits, IKKα and IKKβ, Necessary for IκB Phosphorylation and NF-κB Activation." Cell 91.2 (1997): 243-52. Print.

Zhang, Q., J. A. Didonato, M. Karin, and T. W. Mckeithan. "BCL3 Encodes a Nuclear Protein Which Can Alter the Subcellular Location of NF-kappa B Proteins." Molecular and Cellular Biology Mol. Cell. Biol. 14.6 (1994): 3915-926. Print.

Zhang, M. Y., Harhaj, E. W., Bell, L., Sun, S. C., & Miller, B. A. (1998). Bcl-3 expression and nuclear translocation are induced by granulocyte- macrophage colony-stimulating factor and erythropoietin in proliferating human erythroid precursors. Blood, 92(4), 1225-1234.